

# Light nuclei of even mass number in the Skyrme model

R. A. Battye,<sup>1,\*</sup> N. S. Manton,<sup>2,†</sup> P. M. Sutcliffe,<sup>3,‡</sup> and S. W. Wood<sup>2,§</sup>

<sup>1</sup>*Jodrell Bank Centre for Astrophysics, University of Manchester, Manchester M13 9PL, United Kingdom*

<sup>2</sup>*Department of Applied Mathematics and Theoretical Physics, University of Cambridge, Wilberforce Road, Cambridge CB3 0WA, United Kingdom*

<sup>3</sup>*Department of Mathematical Sciences, Durham University, South Road, Durham DH1 3LE, United Kingdom*

(Received 28 May 2009; published 29 September 2009)

We consider the semiclassical rigid-body quantization of Skyrme solutions of mass numbers  $B = 4, 6, 8, 10$ , and 12. We determine the allowed quantum states for each Skyrme solution and find that they often match the observed states of nuclei. The spin and isospin inertia tensors of these Skyrme solutions are accurately calculated for the first time and are used to determine the excitation energies of the quantum states. We calculate the energy level splittings, using a suitably chosen parameter set for each mass number. We find good qualitative and encouraging quantitative agreement with experiment. In particular, the rotational bands of beryllium-8 and carbon-12, along with isospin 1 triplets and isospin 2 quintets, are especially well reproduced. We also predict the existence of states that have not yet been observed and make predictions for the unknown quantum numbers of some observed states.

DOI: 10.1103/PhysRevC.80.034323

PACS number(s): 12.39.Dc, 11.15.Kc, 21.10.Hw

## I. INTRODUCTION

The SU(2) Skyrme model provides a geometrical picture of nuclear physics in which nuclei are identified with the topological soliton solutions of the model, known as Skyrme solutions [1]. The model has several advantages over conventional nuclear models. First, single Skyrme solutions, which are identified with nucleons, are found to merge to some extent and to lose their individual identities in the solutions describing larger nuclei. This captures an important feature of nuclei with individual nucleons close together and is something that cannot be achieved in conventional point nucleon models. Second, the Skyrme Lagrangian is defined in terms of only three parameters. For each mass number  $B$  we fit these parameters to the mass and size of the nucleus of zero isospin that has mass number  $B$  to obtain predictions with reasonable quantitative accuracy. This is unlike potential and shell-model calculations that require many finely tuned parameters.

The model is a pion field theory and is an extension of the nonlinear  $\sigma$  model. The pion fields  $\pi(x)$  are combined into an SU(2)-valued scalar field, the Skyrme field

$$U(x) = \sigma(x)1_2 + i\pi(x) \cdot \tau, \quad (1)$$

where  $\tau$  denotes the triplet of Pauli matrices and  $\sigma^2 + \pi \cdot \pi = 1$ . The Lagrangian density is [2]

$$\begin{aligned} \mathcal{L} = & \frac{F_\pi^2}{16} \text{Tr} \partial_\mu U \partial^\mu U^\dagger + \frac{1}{32e^2} \text{Tr} [\partial_\mu U U^\dagger, \partial_\nu U U^\dagger] \\ & \times [\partial^\mu U U^\dagger, \partial^\nu U U^\dagger] + \frac{1}{8} m_\pi^2 F_\pi^2 \text{Tr} (U - 1_2), \end{aligned} \quad (2)$$

where  $F_\pi$  is the pion decay constant,  $e$  is a dimensionless parameter, and  $m_\pi$  is the pion mass. Using energy and

length units of  $F_\pi/4e$  and  $2/eF_\pi$ , respectively, the Skyrme Lagrangian can be rewritten as

$$\begin{aligned} L = & \int \left\{ -\frac{1}{2} \text{Tr} (R_\mu R^\mu) + \frac{1}{16} \text{Tr} ([R_\mu, R_\nu][R^\mu, R^\nu]) \right. \\ & \left. + m^2 \text{Tr} (U - 1_2) \right\} d^3x, \end{aligned} \quad (3)$$

where  $R_\mu = \partial_\mu U U^\dagger$  and the dimensionless pion mass  $m = 2m_\pi/eF_\pi$ . As usual, the Lagrangian splits into kinetic and potential parts as  $L = T - V$ , with  $T$  quadratic in the time derivative of the Skyrme field. The potential energy  $V$  is given by

$$\begin{aligned} V = & \int \left\{ -\frac{1}{2} \text{Tr} (R_i R_i) - \frac{1}{16} \text{Tr} ([R_i, R_j][R_i, R_j]) \right. \\ & \left. - m^2 \text{Tr} (U - 1_2) \right\} d^3x. \end{aligned} \quad (4)$$

The Skyrme solutions are minima of the potential energy and are static. They are labeled by their topological charge,  $B$ , the degree of the map  $U : \mathbb{R}^3 \rightarrow \text{SU}(2)$ , which is well-defined provided  $U \rightarrow 1_2$  at spatial infinity and is given by the integral

$$B = \int B_0(x) d^3x, \quad (5)$$

where

$$B_\mu(x) = \frac{1}{24\pi^2} \epsilon_{\mu\nu\alpha\beta} \text{Tr} (\partial^\nu U U^\dagger \partial^\alpha U U^\dagger \partial^\beta U U^\dagger). \quad (6)$$

We denote the minimized potential energy by  $\mathcal{M}_B$ . One interprets a charge  $B$  Skyrme solution, after quantization, as a nucleus of mass number  $B$ . In this picture, nucleons and nuclei arise purely from the pion field and no explicit nucleonic sources are needed.

It is necessary to semiclassically quantize the Skyrme solutions as rigid bodies. The Skyrme Lagrangian is invariant under

\*Richard.Battye@manchester.ac.uk

†N.S.Manton@damtp.cam.ac.uk

‡P.M.Sutcliffe@durham.ac.uk

§S.W.Wood@damtp.cam.ac.uk

rotations in space. It is also invariant under the transformations  $U \rightarrow AUA^\dagger$ , where  $A \in \text{SU}(2)$ . This is isospin symmetry. The rotational and isorotational degrees of freedom are treated as collective coordinates and the Skyrmions are quantized in their rest frame by canonical methods. In this way the Skyrmions acquire spin and isospin. An advantage of this model over other nuclear models that involve collective rotational motion is that it incorporates isospin excitations. In the Skyrme model, the vacuum solution  $U = 1_2$  is isospin invariant, but for each classical Skyrme solution, isospin symmetry as well as rotational symmetry is spontaneously broken. These symmetries are restored by the collective coordinate quantization.

The kinetic energy of a rigidly rotating Skyrme (ignoring the rather trivial translational motion) is of the form

$$T = \frac{1}{2}a_i U_{ij} a_j - a_i W_{ij} b_j + \frac{1}{2}b_i V_{ij} b_j, \quad (7)$$

where  $b_i$  and  $a_i$  are the angular velocities in space and isospace, respectively, and  $U_{ij}$ ,  $V_{ij}$ , and  $W_{ij}$  are inertia tensors [3,4]. The momenta conjugate to  $b_i$  and  $a_i$  are the body-fixed spin and isospin operators  $L_i$  and  $K_i$ . The quantum Hamiltonian  $H$  is obtained by re-expressing  $T$  in terms of these operators. The space-fixed spin and isospin operators are denoted  $J_i$  and  $I_i$ , respectively. Note that  $\mathbf{J}^2 = \mathbf{L}^2$  and  $\mathbf{I}^2 = \mathbf{K}^2$ .

Finkelstein and Rubinstein showed that it is possible to quantize a  $B = 1$  Skyrme as a fermion and showed that for even (odd)  $B$  the spin and isospin are integers (half-integers) [5]. Discrete symmetries of the classical Skyrme solutions<sup>1</sup> give rise to further Finkelstein–Rubinstein (FR) constraints on the space of quantum states  $|\Psi\rangle$ . These constraints are of the form

$$e^{i\theta_2 \mathbf{n}_2 \cdot \mathbf{L}} e^{i\theta_1 \mathbf{n}_1 \cdot \mathbf{K}} |\Psi\rangle = \chi_{\text{FR}} |\Psi\rangle, \quad (8)$$

where  $\mathbf{n}_1, \mathbf{n}_2$  and  $\theta_1, \theta_2$  are, respectively, the axes and angles defining the rotations in isospace and space associated with a particular symmetry, and  $\chi_{\text{FR}} = \pm 1$ . The FR signs,  $\chi_{\text{FR}}$ , define a one-dimensional representation of the symmetry group of the Skyrme. Krusch has found a convenient way to calculate them [6], and we use this method here. A basis for the wave functions  $|\Psi\rangle$  is given by the products  $|J, L_3\rangle \otimes |I, K_3\rangle$ , the tensor products of states for a rigid body in space, and a rigid body in isospace.  $J$  and  $I$  are the total spin and isospin quantum numbers and  $L_3$  and  $K_3$  the projections on to the third body-fixed axes, and the space projection labels (which are the physical third components of spin and isospin) are suppressed. The FR constraints allow only a subset of these products as physical states. A parity operator is introduced by considering a Skyrme's reflection symmetries. Quantum states are therefore labeled by the usual quantum numbers: spin-parity  $J^\pi$  and isospin  $I$ .

The inclusion of the third term in the Lagrangian density, which involves the pion mass, has a significant effect on the

shapes and symmetries of the classical Skyrme solutions. This effect is more marked for larger values of  $B$ . For zero pion mass, the Skyrmions with  $B$  up to 22 and beyond resemble hollow polyhedra, with their baryon density concentrated in a shell of roughly constant thickness, surrounding a region in which the baryon density is very small [7]. This disagrees with the approximately uniform baryon density observed in the interior of real nuclei. Fortunately, it has been established that the hollow polyhedral solutions for  $B \geq 8$  do not remain stable when the pion mass is set at a physically reasonable value, with  $m \approx 1$  [8]. This is because in the interior of the hollow polyhedra the Skyrme field is very close to  $U = -1_2$ , and here the pion mass term gives the field a maximal potential energy and hence instability. This instability results in the interior region splitting into separate smaller subregions. The stable Skyrme solutions are found to exhibit clustering: small Skyrme solutions, such as the cubically symmetric  $B = 4$  solution, appear as substructures within larger solutions [9]. This is a very encouraging development as it has been believed for some time that  $\alpha$  particles exist as stable substructures inside heavier nuclei. The most remarkable success of the  $\alpha$ -particle model is in its prediction for the binding energies of nuclei that can be formed out of an integral number of  $\alpha$  particles.

In earlier work, the  $B = 4, 6$ , and  $8$  Skyrmions have been quantized [4,10], using some approximations to the Skyrme solutions based on the rational map ansatz [11]. The inertia tensors used had the right symmetries but not the correct numerical values. In this article we consider the  $B = 4, 6, 8, 10$ , and  $12$  Skyrmions, using a consistent numerical scheme to recalculate all these solutions. Each of these Skyrmions can be viewed as being built up from  $B = 4$  cubes (it is possible to regard the  $B = 6$  Skyrme as being made up of a  $B = 4$  cube and a  $B = 2$  torus, and the  $B = 10$  solution as consisting of two  $B = 4$  cubes together with two  $B = 1$  Skyrmions). We numerically relax field configurations to the stable Skyrmions, for various values of the dimensionless pion mass  $m$ , and then compute their static energies  $\mathcal{M}_B$ , charge radii  $\langle r^2 \rangle^{1/2}$ , and inertia tensors. Appendix A tabulates the calculated numerical values for  $m = 0.5, 1$ , and  $1.5$  and Appendix B describes the quadratic interpolation method used to estimate these quantities for any given  $m$ . In the next section we describe our method of choosing  $m$  and of calibrating the model to ensure that it provides quantitatively accurate predictions of nuclear properties.

For each Skyrme we determine all the FR-allowed quantum states and their excitation energies, working up to spin and isospin values just beyond the edge of what is experimentally accessible. Our rigid-body quantization leads to an infinite tower of quantum states (the  $B = 1$  Skyrme, for example, has quantum states for all half-integer values of spin). However, in practice we expect a Skyrme to deform as it spins (this is known to occur for the  $B = 1$  Skyrme [12]), and this disallows many higher-spin states. We are therefore not concerned that in some cases we predict higher-spin states that are not experimentally observed. It is also possible that a Skyrme might break up as it spins, a phenomenon that is known to occur for real nuclei.

<sup>1</sup>Only the  $B = 1$  and  $B = 2$  Skyrmions possess continuous symmetries.

TABLE I. Experimental data and calibration for each  $B$ .

$B$	Nucleus	Mean charge radius (fm)	Mass (MeV)	$m$	Length scale $2/eF_\pi$ (fm)	Classical energy scale $F_\pi/4e$ (MeV)	Quantum energy scale $e^3 F_\pi$ (MeV)
4	$^4\text{He}$	1.71	3727	0.820	1.173	6.169	4588
6	$^6\text{Li}$	2.55	5601	1.153	1.648	5.752	2492
8	$^8\text{Be}$	2.51	7455	0.832	1.190	6.336	4339
10	$^{10}\text{B}$	2.58	9324	0.830	1.187	6.348	4354
12	$^{12}\text{C}$	2.46	11175	0.685	0.980	6.525	6216

## II. CALIBRATION

The model was first calibrated by Adkins, Nappi, and Witten, by fitting the model in the  $B = 1$  sector to the masses of the proton and  $\Delta$  resonance [13,14]. In a recent article a new calibration was obtained by equating the mass and size of the quantized  $B = 6$  Skyrmion to the mass and size of the lithium-6 nucleus [10]. However this was performed using the approximate Skyrmion found using the rational map ansatz. Evidently, there are many possible ways in which the model may be calibrated.

The three parameters of the model are the pion decay constant  $F_\pi$  (experimentally 186 MeV), the pion mass  $m_\pi$  (experimentally 138 MeV), and the dimensionless parameter  $e$ . Strictly speaking, one may argue that we are only free to set  $e$ , as the other constants are fixed by experiment. However, we consider it permissible to vary  $F_\pi$ , as we consider it to be a renormalized pion decay constant. We also allow  $e$  to vary with mass number,  $e = e(B)$ , to get better agreement with experiment. The length and classical energy scales are  $2/eF_\pi$  and  $F_\pi/4e$ , respectively. For the “nuclear” variant of the model the value of  $e$  is less than its value for the  $B = 1$  case (4.84 [14]). This effectively takes into account nonzero mode motion of Skyrmions that leads to an increase in the sizes of the classical configurations. We recall that the quantum Hamiltonian for a rigidly rotating body is equal to the squared angular momentum operator divided by twice the moment of inertia of the body [15]. The moment of inertia has units equal to the mass scale multiplied by the square of the length scale:  $(F_\pi/4e) \times (2/eF_\pi)^2 = 1/e^3 F_\pi$ . The quantum energy scale is its reciprocal,  $e^3 F_\pi$ . The total energy of a quantum state of a Skyrmion is therefore equal to  $(F_\pi/4e)\mathcal{M}_B + e^3 F_\pi E_Q$ , where  $E_Q$  is the quantum kinetic energy of the state. The ratio of the total energy of a quantum state to the classical energy of the Skyrmion is  $1 + 4e^4(E_Q/\mathcal{M}_B)$ . The ratios of the quantum energies of Skyrmion states are therefore sensitive to the value of  $e$ .

The classical Skyrmion solutions match the experimental pion tails of nuclei if we use the physical value of  $m_\pi$  of 138 MeV. For this reason, we keep  $m_\pi$  fixed at this value. For each  $B$ , we choose  $m$  (and therefore fix the length scale, as  $m = 2m_\pi/eF_\pi$ ) such that the calculated mean charge radius agrees with that of the nucleus with zero isospin with this value of  $B$ . Within the Skyrme model, the mean charge radius of a

nucleus with zero isospin is estimated to be the square root of

$$\langle r^2 \rangle = \frac{\int r^2 B_0(x) d^3x}{\int B_0(x) d^3x}, \quad (9)$$

because the electric charge density is half the baryon density [10]. Having fixed the length scales, we then set the classical energy scales such that the sum of the static Skyrmion masses and spin contributions agree with the nuclear masses. A more refined analysis would take into account loop corrections and Casimir energy contributions to the static Skyrmion masses. These contributions have been estimated for the  $B = 1$  case [16] but not for higher baryon numbers. It is found that in each case  $m$  takes a value between 0.6 and 1.2. The experimental data, the values of  $m$  used, and the length and energy scales are listed in Table I.<sup>2</sup> Table II lists the corresponding Skyrme parameters.

A larger length scale, for example in the case of  $B = 6$ , takes into account loose vibrational motion and leads to larger moments of inertia, which is desirable. The small length scale for  $B = 12$  takes into account the compact size of the carbon-12 nucleus. Another reason to use separate parameter sets for each  $B$  comes from comparing the rotational bands of beryllium-8 and carbon-12. These nuclei have  $0^+$  ground states and  $2^+$  and  $4^+$  excited states, at 3.0 and 11.4 MeV, respectively, for beryllium-8 and at 4.4 and 14.4 MeV, respectively, for carbon-12. Naively, one might expect carbon-12 to be larger and heavier than beryllium-8 (in dimensionless units, the  $B = 12$  Skyrmion is larger in size and has a larger classical mass

<sup>2</sup>The mean charge radius of beryllium-8 has not been measured due to its instability. Here we use the value for its isobar, lithium-8.

TABLE II. Optimized Skyrme parameters for each  $B$ .

$B$	$e$	$F_\pi$ (MeV)
4	3.80	91.1
6	4.35	74.2
8	3.88	91.7
10	3.88	91.9
12	3.58	102.5

than the  $B = 8$  Skyrmion) and for it therefore to have a larger moment of inertia. As the moment of inertia appears in the denominator of the quantum Hamiltonian, this would lead to carbon-12 having a smaller rotational band splitting than that of beryllium-8, which is not the case. Evidently, the only way to deal with this problem in our model is to use a different parameter set for each. Experimentally, the mean charge radii of the nuclei we are considering are approximately constant for  $6 \leq B \leq 12$ , whereas the dimensionless Skyrmion mean charge radius increases with  $B$ . The optimized parameter sets allow us to keep the nuclear mean charge radii approximately constant.

### III. $B = 4$

The minimal-energy  $B = 4$  Skyrmion has octahedral symmetry and a cubic shape. A surface of constant baryon density is presented in Fig. 1. The color scheme represents the direction in isospace of the associated pion fields. For regions in space where at least one of the pion fields does not vanish, the normalized pion field  $\hat{\pi}$  can be defined and takes values in the unit sphere. We color this sphere by making a region close to the north pole white and a region close to the south pole black. On an equatorial band, where  $\hat{\pi}_3$  is small, we divide the sphere into three segments and color these red, blue, and green. In Fig. 1, opposite faces share the same color and vertices alternate between black and white.

For a derivation of the Skyrmion's quantum states we refer the reader to Ref. [4], and here we only state the main results. For an earlier discussion, see Ref. [17]. The rotational symmetry group of the Skyrmion,  $O_h$ , is one of the largest point symmetry groups. This leads to particularly restrictive FR constraints on the space of allowed states. The  $O_h$  symmetry implies that the inertia tensors are diagonal with  $U_{11} = U_{22}$  and  $U_{33}$  different,  $V_{ij}$  proportional to the identity matrix, and  $W_{ij} = 0$ . The quantum collective coordinate Hamiltonian is therefore the sum of a spherical top in space and a symmetric top in isospace,

$$H = \frac{1}{2V_{33}}\mathbf{J}^2 + \frac{1}{2U_{11}}\mathbf{I}^2 + \left( \frac{1}{2U_{33}} - \frac{1}{2U_{11}} \right) K_3^2. \quad (10)$$

The inertia tensors are given in Appendix A1. The lowest state is a  $0^+$  state with isospin 0, which has the quantum

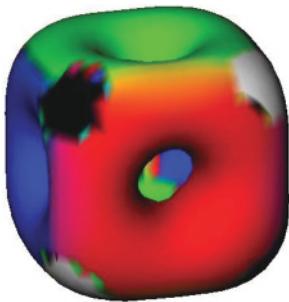


FIG. 1. (Color online) A surface of constant baryon density for the  $B = 4$  Skyrmion. Different colors indicate different directions of the pion fields.

TABLE III. Energy levels of the quantized  $B = 4$  Skyrmion.

$I$	$J^\pi$	$E (\times 10^{-4})$	$E$ (MeV)
0	$0^+$	0.0	0.0
	$4^+$	129.7	59.5
1	$2^-$	94.1	43.2

numbers of the  $\alpha$ -particle in its ground state. The first excited state with isospin 0 is a  $4^+$  state, which has not been experimentally observed, because of its high energy. The lowest state with isospin 1 is a  $2^-$  state, which matches the observed isotriplet, including the hydrogen-4 and lithium-4 ground states. The energy levels are given in Table III. Only the quantized kinetic contributions to the total energies are listed; the static Skyrmion mass must be added to give the total energy. For example, the ground state has zero kinetic energy and therefore its total energy is precisely 3727 MeV, as given in Table I. The  $4^+$  state has additional kinetic energy of  $10/V_{33} = 129.7 \times 10^{-4}$  in dimensionless units. In the final column of Table III we list the values in physical units, using the  $B = 4$  conversion factor  $e^3 F_\pi = 4588$  MeV given in Table I. We overpredict the excitation energy of the  $2^-$  isotriplet as 43.2 MeV compared with an average experimental value of 23.7 MeV [18].

In summary, the ground state of helium-4 and the isotriplet of  $2^-$  states arise as quantum states of the  $B = 4$  Skyrmion. The cubic shape of the Skyrmion may become deformed as it spins. It may be for this reason that the  $4^+$  state is not observed experimentally.

### IV. $B = 6$

The  $B = 6$  Skyrmion has  $D_{4d}$  symmetry (see Fig. 2). We refer the reader to Ref. [4] for a discussion of its quantization. The quantum Hamiltonian is that of a system of coupled symmetric tops:

$$H = \frac{1}{2V_{11}}\mathbf{J}^2 + \frac{1}{2U_{11}}\mathbf{I}^2 + \left( \frac{U_{33}}{2\Delta_{33}} - \frac{1}{2V_{11}} \right) L_3^2 + \left( \frac{V_{33}}{2\Delta_{33}} - \frac{1}{2U_{11}} \right) K_3^2 + \frac{W_{33}}{\Delta_{33}} L_3 K_3, \quad (11)$$

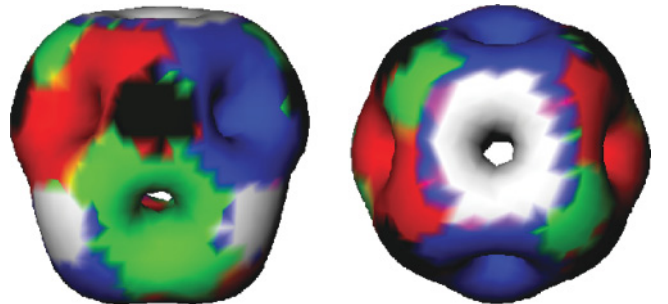


FIG. 2. (Color online) A surface of constant baryon density for the  $B = 6$  Skyrmion (two viewpoints).

TABLE IV. Energy levels of the quantized  $B = 6$  Skyrmion.

$I$	$J^\pi$	Quantum state	$E (\times 10^{-4})$	$E$ (MeV)
0	$1^+$	$ 1, 0\rangle \otimes  0, 0\rangle$	6.5	1.6
	$3^+$	$ 3, 0\rangle \otimes  0, 0\rangle$	38.9	9.7
	$4^-$	$( 4, 4\rangle -  4, -4\rangle) \otimes  0, 0\rangle$	73.5	18.3
	$5^+$	$ 5, 0\rangle \otimes  0, 0\rangle$	97.3	24.2
	$5^-$	$( 5, 4\rangle +  5, -4\rangle) \otimes  0, 0\rangle$	105.9	26.4
1	$0^+$	$ 0, 0\rangle \otimes  1, 0\rangle$	47.4	11.8
	$2^+$	$ 2, 2\rangle \otimes  1, 1\rangle +  2, -2\rangle \otimes  1, -1\rangle$	62.6	15.6
		$ 2, 0\rangle \otimes  1, 0\rangle$	66.8	16.7
	$2^-$	$ 2, 2\rangle \otimes  1, -1\rangle +  2, -2\rangle \otimes  1, 1\rangle$	73.1	18.2
	$3^+$	$ 3, 2\rangle \otimes  1, 1\rangle -  3, -2\rangle \otimes  1, -1\rangle$	82.0	20.4
	$3^-$	$ 3, 2\rangle \otimes  1, -1\rangle -  3, -2\rangle \otimes  1, 1\rangle$	92.5	23.1
	$4^+$	$ 4, 2\rangle \otimes  1, 1\rangle +  4, -2\rangle \otimes  1, -1\rangle$	108.0	26.9
		$ 4, 0\rangle \otimes  1, 0\rangle$	112.2	28.0
	$4^-$	$ 4, 2\rangle \otimes  1, -1\rangle +  4, -2\rangle \otimes  1, 1\rangle$	118.5	29.5
		$( 4, 4\rangle +  4, -4\rangle) \otimes  1, 0\rangle$	120.9	30.1
2	$0^-$	$ 0, 0\rangle \otimes ( 2, 2\rangle -  2, -2\rangle)$	137.4	34.2
	$1^+$	$ 1, 0\rangle \otimes  2, 0\rangle$	148.6	37.0
	$1^-$	$ 1, 0\rangle \otimes ( 2, 2\rangle +  2, -2\rangle)$	143.9	35.9
	$2^+$	$ 2, 2\rangle \otimes  2, 1\rangle -  2, -2\rangle \otimes  2, -1\rangle$	157.3	39.2
	$2^-$	$ 2, 0\rangle \otimes ( 2, 2\rangle -  2, -2\rangle)$	156.9	39.1
		$ 2, 2\rangle \otimes  2, -1\rangle -  2, -2\rangle \otimes  2, 1\rangle$	167.8	41.8

where  $\Delta_{33} = U_{33}V_{33} - W_{33}^2$ . Its allowed quantum states are listed in Table IV, together with their energy levels computed using the inertia tensors in Appendix A2.

The Skyrme model qualitatively reproduces the experimental spectrum of lithium-6 and its isobars and predicts some further states, including  $J^\pi = 4^-, 5^+$ , and  $5^-$  excited states of lithium-6 with isospin 0. The ground state of lithium-6 is

correctly predicted to be a  $1^+$  state (Fig. 3). We also find a  $3^+$  excited state, which is seen experimentally. However, we overpredict its excitation energy by roughly a factor of 5. The model does not account for centrifugal stretching nor the allowed decay of the  $3^+$  state to an  $\alpha$ -particle plus a deuteron, which may be the reason for our overprediction. The lowest allowed state with isospin 1 is a  $0^+$  state, which is seen

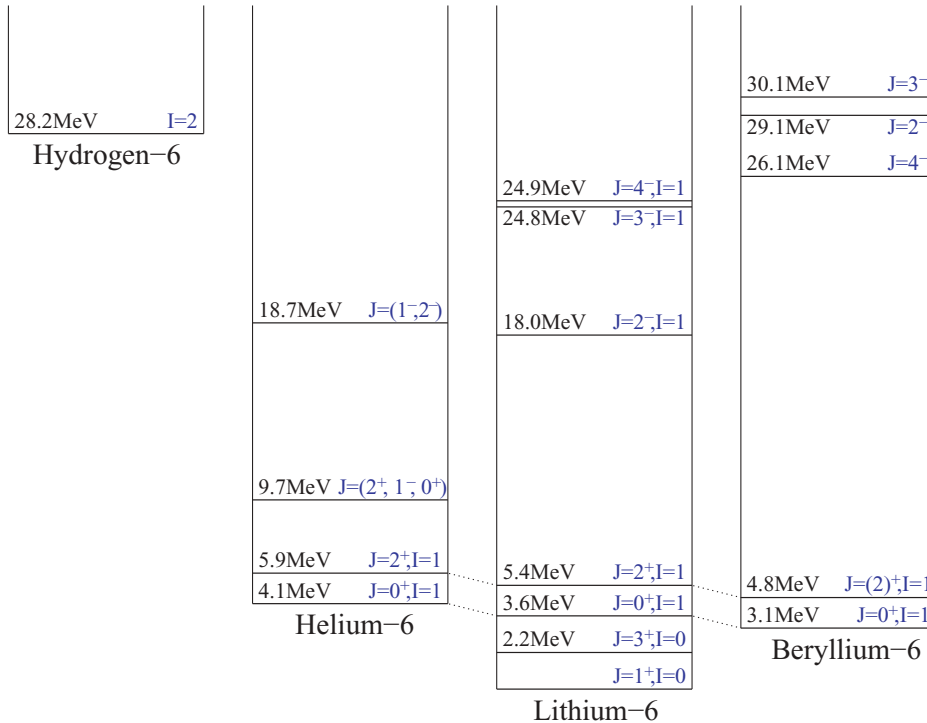


FIG. 3. (Color online) Energy level diagram for nuclei of mass number 6. Mass splittings between nuclei are adjusted to eliminate the proton/neutron mass difference and remove Coulomb effects, as described in Ref. [19].



experimentally as an isotriplet that includes the helium-6 and beryllium-6 ground states. An excited  $2^+$  state of this isotriplet exists, which we also find within our model. However, again we overpredict its excitation energy. We predict an additional  $2^+$  state with isospin 1. The lowest allowed negative-parity state with isospin 1 is predicted to be a  $2^-$  state with excitation energy 18.2 MeV. We therefore suggest that the observed 9.7 MeV state of helium-6 is our second  $2^+$  state. Lithium-6 has a  $2^-$  state with isospin 1 at 18.0 MeV. We predict that the 18.7 MeV state of helium-6 has  $J^\pi = 2^-$  and is one of its isotriplet partners. A  $2^-$  state of beryllium-6 is observed at 29.1 MeV. Perhaps this state completes the isotriplet, but its high energy makes this unclear. States of lithium-6 and beryllium-6 with  $J^\pi = 3^-$  and  $4^-$  and with isospin 1 have been experimentally observed. We predict these states with roughly the correct excitation energies. We also predict the existence of  $3^+$  and  $4^+$  states with isospin 1, which have not been seen experimentally. The ground state of hydrogen-6 has isospin 2, at 28.2 MeV above the lithium-6 ground state, and an undetermined spin. The Skyrme model gives the lowest allowed state with isospin 2 as a  $0^-$  state, and its excitation energy is 34.2 MeV. Higher spin excited isospin 2 states are also allowed in the model, but they have not been experimentally observed.

In summary, the quantum numbers of the low-lying states of the  $B = 6$  Skyrmon agree with those of the nuclei of mass number 6, although we overpredict their excitation energies. Our calculated values for the excitation energies of the isospin 1 states are, however, quantitatively good. We have also made predictions for the spins of two excited states of helium-6 and predict that the hydrogen-6 ground state is a  $0^-$  state.

## V. $B = 8$

When  $m = 1$ , the stable  $B = 8$  Skyrmon is  $D_{4h}$ -symmetric and resembles two touching  $B = 4$  cubes, matching the  $\alpha$ -particle model picture of beryllium-8 as an almost bound configuration of two  $\alpha$  particles. A surface of constant baryon density is displayed in Fig. 4. In Ref. [4] we approximated the  $B = 8$  Skyrmon as a “double cube” of two  $B = 4$  Skyrmons and made estimates for its inertia tensors, enabling us to estimate its energy levels. We refer the reader to this article for a discussion of its quantization. The quantum Hamiltonian is the sum of a symmetric top in space and an asymmetric top in

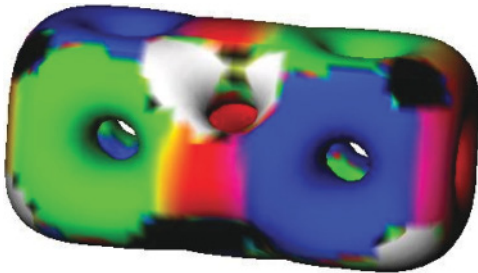


FIG. 4. (Color online) A surface of constant baryon density for the  $B = 8$  Skyrmon, resembling two  $B = 4$  cubes.

TABLE V. Energy levels of the quantized  $B = 8$  Skyrmon.  $n$  is the number of FR-allowed states with given  $I$  and  $J^\pi$ .

$I$	$J^\pi$	$n$	$E (\times 10^{-4})$	$E$ (MeV)
0	$0^+$	1	0.0	0.0
	$2^+$	1	7.0	3.0
	$4^+$	2	23.4, 56.1	10.2, 24.3
1	$0^-$	1	30.0	13.0
	$2^+$	1	44.6	19.3
	$2^-$	2	37.1, 46.3	16.1, 20.1
	$3^+$	1	51.6	22.4
	$3^-$	1	53.3	23.1
	$4^+$	1	61.0	26.5
	$4^-$	3	53.5, 62.7, 86.2	23.2, 27.2, 37.4
2	$0^+$	2	87.6, 93.5	38.0, 40.6
	$0^-$	1	90.9	39.5
	$2^+$	3	94.6, 100.5, 108.1	41.0, 43.6, 46.9
	$2^-$	2	98.0, 103.0	42.5, 44.7

isospace:

$$H = \frac{1}{2V_{11}}\mathbf{J}^2 + \left( \frac{1}{2V_{33}} - \frac{1}{2V_{11}} \right) L_3^2 + \frac{1}{2U_{11}}K_1^2 + \frac{1}{2U_{22}}K_2^2 + \frac{1}{2U_{33}}K_3^2. \quad (12)$$

The exact inertia tensors are given in Appendix A3. As anticipated on symmetry grounds, the inertia tensor  $U_{ij}$  has three distinct eigenvalues (the earlier double cube estimate made two of them equal). The energy levels calculated using the exact inertia tensors are listed in Table V.

Figure 5 is an energy level diagram for nuclei of mass number 8. The Skyrme model predictions for positive-parity states agree well with experiment. The ground state of beryllium-8 is correctly determined to be a  $0^+$  state. The rotational band of beryllium-8 is remarkably well reproduced in our model: we predict the  $2^+$  and  $4^+$  states at 3.0 and 10.2 MeV, respectively, which is very close to the experimental values of 3.0 and 11.4 MeV, respectively. We predict a second  $4^+$  state with isospin 0 at 24.3 MeV. Experimentally, beryllium-8 has two further  $4^+$  states with isospin 0 (at 19.9 and 25.5 MeV).

The model predicts that the lowest allowed state with isospin 1 has  $J^\pi = 0^-$ . However, the ground states of lithium-8 and boron-8 are believed to have  $J^\pi = 2^+$ . Perhaps the  $0^-$  isotriplet may be seen experimentally in the future, for it is known that low-lying spin 0, negative-parity states are difficult to observe, as experienced in the search for the bottomonium and charmonium ground state mesons  $\eta_b$  and  $\eta_c$  [21,22]. Our estimate for the excitation energy of the  $2^+$  isotriplet is 19.3 MeV, which experimentally has an average excitation energy of 16.7 MeV. In addition, we predict a  $3^+$  isotriplet at 22.4 MeV, to be compared to the experimental value of 19.0 MeV. The model forbids spin 1 states with isospin 1. However, several  $1^+$  states with isospin 1 have been observed in the spectrum of lithium-8. Perhaps these may arise as quantum states of an alternative  $B = 8$  Skyrmon, or from the

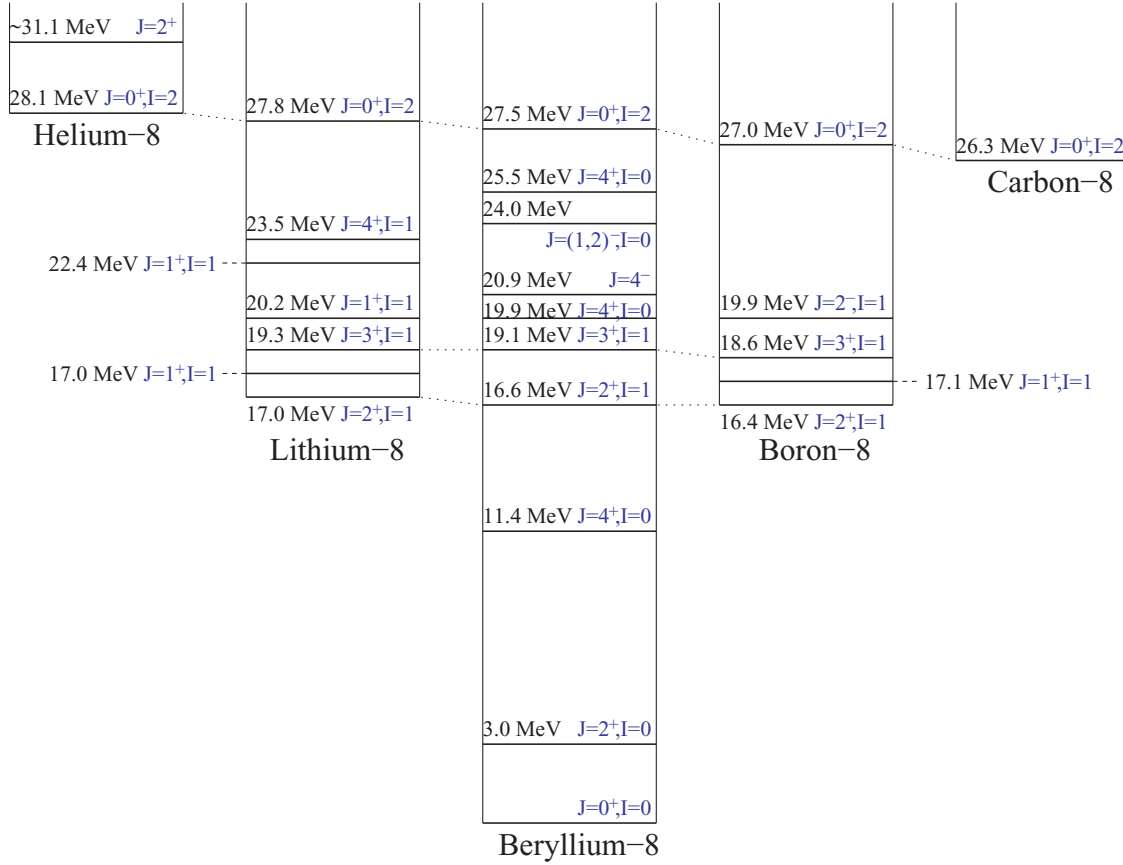


FIG. 5. (Color online) Energy level diagram for nuclei of mass number 8. Mass splittings between nuclei are adjusted to eliminate the proton/neutron mass difference and remove Coulomb effects, as described in Ref. [20].

quantization of further degrees of freedom, such as vibrational modes. We predict two  $2^-$  states with isospin 1 at 16.1 and 20.1 MeV. A state with these quantum numbers has been seen in the spectrum of boron-8 at 19.9 MeV. We predict a  $4^+$  state with isospin 1 at 26.5 MeV, which is seen in the spectrum of lithium-8 at 23.5 MeV, although its beryllium-8 and boron-8 partners are not yet confirmed. Beryllium-8 has a  $4^-$  state at 20.9 MeV, which we identify with our  $4^-$  state with isospin 1 at 23.2 MeV.

We find that the lowest state with isospin 2 has  $J^\pi = 0^+$ . Experimentally this forms an isospin 2 quintet that includes the ground states of helium-8 and carbon-8. We calculate its excitation energy to be 38.0 MeV, to be compared to the experimental value of 27.3 MeV. A  $2^+$  state of helium-8 has been observed at approximately 31.1 MeV, which we predict at 41.0 MeV.

In summary, the spectrum of beryllium-8 is very well reproduced in our model, in particular its isospin 0 rotational band. So too are the experimentally observed isospin 1 triplets and the isospin 2 quintet. Predicted  $0^-$  states with isospin 1 have not been seen in the spectra of nuclei of mass number 8; however, as we mentioned they may be difficult to observe. We have been unable to explain the appearance of  $1^+$  states of lithium-8 and boron-8. We are led to consider refinements of our model and its quantization to address this.

## VI. $B = 10$

In Ref. [8] the minimal-energy solution for  $B = 10$  was found to have  $D_{2h}$  symmetry. This Skyrmion can be thought of within the context of the  $\alpha$ -particle model as a pair of  $B = 4$  cubes with two  $B = 1$  Skyrmions between, as illustrated in Fig. 6.

Here, we quantize this Skyrmion for the first time. We use the rational map ansatz to determine its FR constraints. For an overview of the ansatz, which provides close approximations to the exact Skyrmion solutions, see Ref. [11]. While it does not provide quantitatively exact results, it precisely describes the symmetry group of many Skyrmions and therefore can

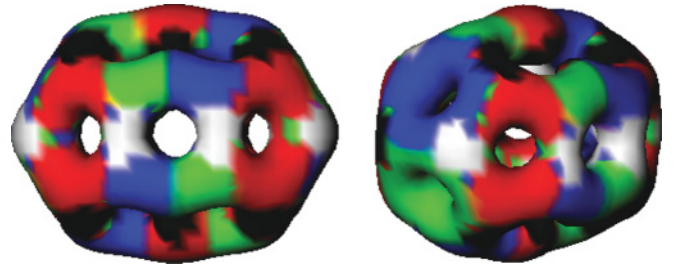


FIG. 6. (Color online) A surface of constant baryon density for the  $B = 10$  Skyrmion (two viewpoints).

be used to derive their FR constraints. In the  $B = 10$  case a suitable rational map is

$$R(z) = \frac{\alpha + \beta z^2 + \gamma z^4 + \delta z^6 + \epsilon z^8 + z^{10}}{1 + \epsilon z^2 + \delta z^4 + \gamma z^6 + \beta z^8 + \alpha z^{10}}, \quad (13)$$

with  $\alpha = 0.28$ ,  $\beta = -9.37$ ,  $\gamma = 14.83$ ,  $\delta = 4.98$ , and  $\epsilon = 3.02$ . The  $D_2$  rotation group is generated by two  $C_2$  symmetries, which correspond to the following symmetries of the rational map:

$$R(-z) = R(z), \quad R(1/z) = 1/R(z). \quad (14)$$

The associated FR constraints are determined using Krusch's method [6] to be

$$e^{i\pi L_3}|\Psi\rangle = |\Psi\rangle, \quad e^{i\pi L_1}e^{i\pi K_1}|\Psi\rangle = -|\Psi\rangle, \quad (15)$$

so the signs  $\chi_{\text{FR}}$  form one of the nontrivial one-dimensional representations of  $D_2$ .

Generally, the parity operator in the Skyrme model is an inversion in space and isospace:  $\mathcal{P} : U(\mathbf{x}) \rightarrow U^\dagger(-\mathbf{x})$ . A rational map is invariant under parity if it satisfies

$$R(-1/\bar{z}) = -1/\overline{R(z)}. \quad (16)$$

For a quantized Skymion described by such a rational map, all states would have positive parity. However, as the rational map (13) satisfies the inversion symmetry

$$R(-1/\bar{z}) = 1/\overline{R(z)}, \quad (17)$$

the parity operation in this case is equivalent to a single rotation in isospace, given by  $\mathcal{P} = e^{i\pi K_3}$ . The parity of a quantum state is its eigenvalue when acted on by this  $\mathcal{P}$ . Note that we attach the parity label to the spin quantum number, to form  $J^\pi$ , as is conventionally done in nuclear physics, despite the fact that in the Skyrme model the parity operator generally reduces to a combination of rotations in space and in isospace.

For the  $B = 10$  Skymion, the symmetries imply that the inertia tensors  $U_{ij}$  and  $V_{ij}$  are diagonal, and the only nonzero component of the mixed inertia tensor  $W_{ij}$  is  $W_{33}$ . The quantum Hamiltonian is that of a system of coupled asymmetric tops:

$$H = \frac{1}{2V_{11}}L_1^2 + \frac{1}{2V_{22}}L_2^2 + \frac{U_{33}}{2\Delta_{33}}L_3^2 + \frac{1}{2U_{11}}K_1^2 + \frac{1}{2U_{22}}K_2^2 + \frac{V_{33}}{2\Delta_{33}}K_3^2 + \frac{W_{33}}{\Delta_{33}}L_3K_3, \quad (18)$$

where  $\Delta_{33} = U_{33}V_{33} - W_{33}^2$  as before. In the absence of symmetry and FR constraints,  $(2J+1) \times (2I+1)$  different nondegenerate levels would correspond to any given pair of  $J$  and  $I$ . Imposing the FR constraints, however, substantially reduces the number of allowed states. The calculation of energy levels is similar to the case of a general asymmetric top, described in Ref. [15]. However, the final term in Eq. (18) mixes states of the form  $|J, L_3\rangle + |J, -L_3\rangle$  and  $|J, L_3\rangle - |J, -L_3\rangle$  (and similarly for isospin basis states). In Table VI we list the total number of allowed states,  $n$ , for different combinations of spin and isospin, together with their energy eigenvalues. The energy levels are calculated by diagonalizing the Hamiltonian in matrix form, separately for each combination of  $J^\pi$  and  $I$ . The precise forms of the

TABLE VI. Energy levels of the quantized  $B = 10$  Skymion.

$I$	$J^\pi$	$n$	$E (\times 10^{-4})$	$E$ (MeV)
0	$1^+$	1	2.5	1.1
	$2^+$	1	6.6	2.9
	$3^+$	2	12.7, 16.1	5.5, 7.0
	$4^+$	2	21.1, 24.3	9.2, 10.6
1	$0^+$	1	23.8	10.4
	$0^-$	1	24.9	10.9
	$1^-$	1	27.5	12.0
	$2^+$	2	30.0, 31.7	13.1, 13.8
	$2^-$	3	31.1, 31.6, 32.8	13.5, 13.8, 14.3
	$3^+$	1	37.8	16.5
	$3^-$	3	37.7, 38.9, 41.1	16.4, 17.0, 17.9
	$4^+$	3	44.4, 46.1, 51.1	19.3, 20.1, 22.2
	$4^-$	5	45.5, 46.2, 47.2, 49.3, 52.2	19.8, 20.1, 20.6, 21.5, 22.7
2	$0^+$	1	76.0	33.1
	$0^-$	1	72.7	31.7
	$1^+$	2	73.9, 78.5	32.2, 34.2
	$1^-$	1	74.0	32.2
	$2^+$	4	78.1, 82.2, 82.7, 83.9	34.0, 35.8, 36.0, 36.5
	$2^-$	3	78.9, 79.2, 80.6	34.4, 34.5, 35.1
	$3^+$	5	84.2, 87.6, 88.7, 90.1, 92.1	36.6, 38.1, 38.6, 39.2, 40.1
	$3^-$	3	85.2, 86.7, 88.6	37.1, 37.8, 38.6
3	$0^+$	2	142.9, 147.5	62.2, 64.2
	$0^-$	2	144.1, 153.2	62.7, 66.7
	$1^+$	1	150.0	65.3
	$1^-$	2	146.8, 155.7	63.9, 67.8
	$2^+$	5	149.1, 150.8, 153.7, 154.2, 155.4	64.9, 65.6, 66.9, 67.1, 67.7
	$2^-$	6	150.0, 151.0, 151.7, 159.3, 159.9, 161.1	65.3, 65.7, 66.1, 69.4, 69.6, 70.1
	$3^+$	4	156.9, 160.2, 161.6, 163.6	68.3, 69.8, 70.3, 71.2
	$3^-$	6	157.0, 157.9, 160.4, 165.9, 167.3, 169.3	68.4, 68.7, 69.8, 72.2, 72.8, 73.7

eigenvectors are omitted as they do not add anything to our discussion.

The ground state of boron-10 has  $J^\pi = 3^+$  and its first excited state has  $J^\pi = 1^+$  at 0.7 MeV (Fig. 7). We incorrectly determine the  $1^+$  state to be the ground state and  $3^+$  states to be excited states. However, this problem arises in other models of boron-10, for example, in models involving nucleon-nucleon potentials in chiral perturbation theory [23]. Boron-10 has further isospin 0 excited states, including  $2^+$ ,  $3^+$ , and  $4^+$  states at 3.6, 4.8, and 6.0 MeV, respectively. We find that our model only allows positive-parity states with isospin 0, and our predictions for the excitation energies of the aforementioned states are of the correct order of magnitude. Second  $3^+$  and  $4^+$  states with isospin 0 are allowed, which we identify with the states of boron-10 at 7.0 and 10.8 MeV, respectively. Curiously,  $2^-$ ,  $3^-$ , and  $4^-$  states of boron-10 with isospin 0 have been found experimentally at 5.1, 6.1, and 6.6 MeV, respectively. Consideration of further degrees of freedom or the quantization of an alternative  $B = 10$  Skymion may be necessary to account for these negative-parity states.



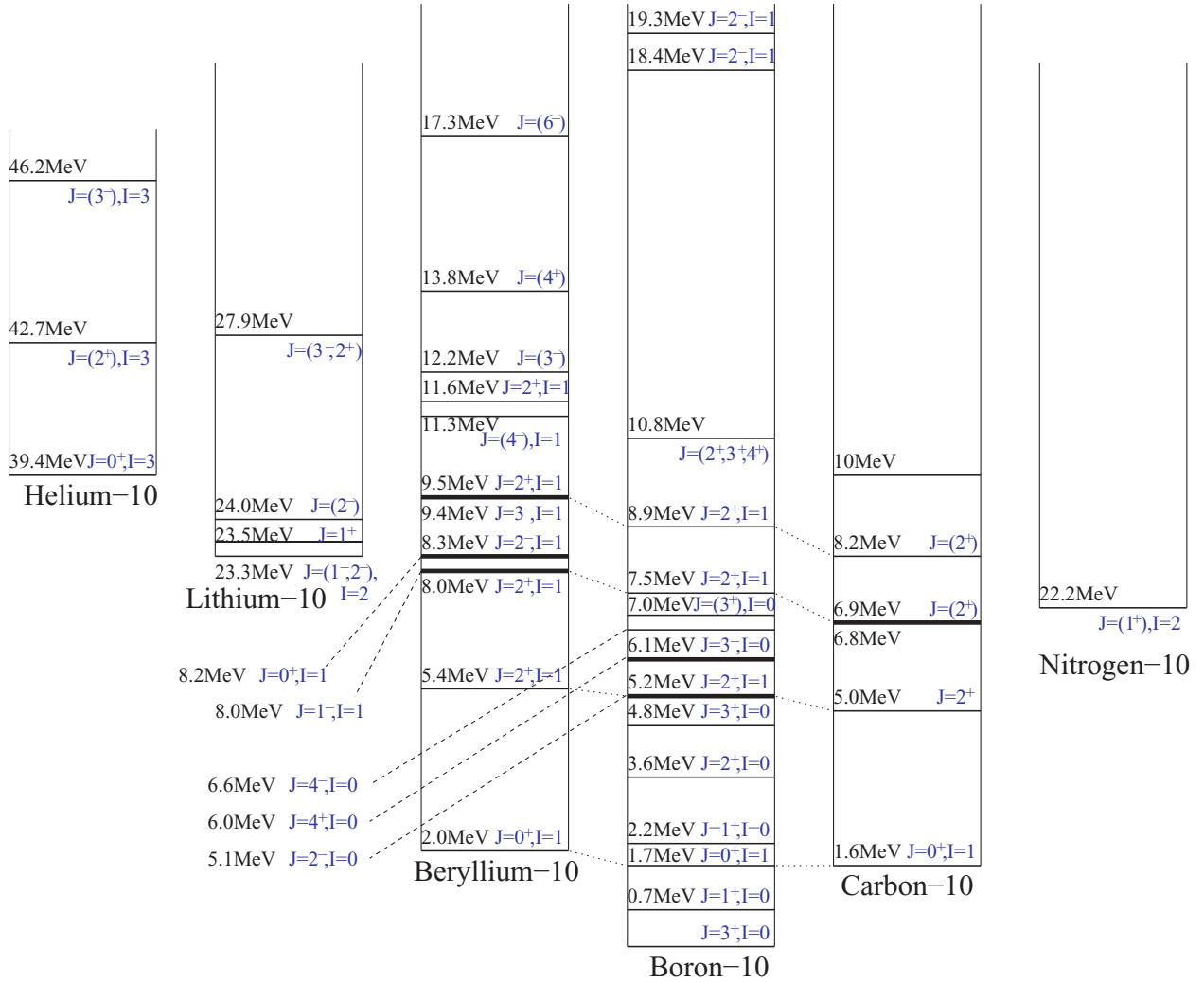


FIG. 7. (Color online) Energy level diagram for nuclei of mass number 10. Individual isobars are shifted vertically for clarity, and mass splittings between nuclei are adjusted to eliminate the proton/neutron mass difference and remove Coulomb effects, as described in Ref. [20].

We find that the lowest allowed state with isospin 1 has  $J^\pi = 0^+$  and is at 4.9 MeV above the lowest  $3^+$  isospin 0 state. Experimentally this is observed as an isospin 1 triplet that includes the beryllium-10 and carbon-10 ground states and has an average excitation energy of 1.8 MeV relative to the boron-10 ground state. Three  $2^+$  spin excitations of this isotriplet have been observed, at average excitation energies 5.2, 7.4, and 8.9 MeV. We predict two such excitations at 7.6 and 8.3 MeV. Note that our model disallows a  $J^\pi = 1^+$  state with isospin 1. This agrees with experimental observations. Additionally,  $1^-$ ,  $2^-$ , and  $3^-$  states with isospin 1 have been seen in the spectrum of beryllium-10, and our predictions for their excitation energies are close to the experimental values. A number of  $2^-$  states with isospin 1 are also seen in the spectrum of boron-10.

For isospins 2 and 3, we find that all possible spins and parities are allowed and that in both cases the lowest state is a  $0^+$  state. The spins of the lithium-10 and nitrogen-10 states (both with isospin 2) are not well established. The lowest state of lithium-10 is at 23.3 MeV above that of boron-10, and its

spin is uncertain: either  $1^-$  or  $2^-$ . We calculate these states to exist at 26.7 and 28.8 MeV above the lowest  $3^+$  isospin 0 state. Lithium-10 has an excited  $1^+$  state, and the lowest state of nitrogen-10 is believed to be a  $1^+$  state. We predict two  $1^+$  states with isospin 2 and slightly overpredict their excitation energies. The lowest helium-10 state is a  $0^+$  state at 39.4 MeV above the boron-10 ground state. This is to be compared to our value of 56.7 MeV. In our model, the isobar splittings increase in proportion to  $I(I+1)$ . However, as can be seen from the nuclear energy level diagrams, this approximately quadratic behavior is not precisely reflected in the data.

In summary, the quantum numbers and excitation energies of the states of nuclei of mass number 10 are reasonably well described by our model. However, the appearance of a  $1^+$  state as the isospin 0 ground state disagrees with that of boron-10, but as we mentioned this is a well-known artifact of nuclear models. The negative-parity states with isospin 0 in the nuclear spectra may arise as quantum states of an alternative  $B = 10$  Skyrmin, invariant under an alternative symmetry group that may permit such states. We find significantly more

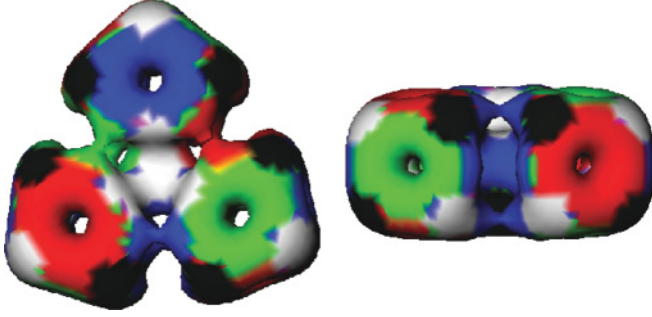


FIG. 8. (Color online) A surface of constant baryon density for the  $D_{3h}$ -symmetric  $B = 12$  Skyrmion (two viewpoints).

allowed states with isospins 2 and 3 than have been found experimentally. However, we are not too concerned about those of higher spin, as the  $D_{2h}$  symmetry may become deformed as the Skyrmin spins.

### VII. $B = 12$

In the  $\alpha$ -particle model, the classical minimum of the potential energy for three  $\alpha$  particles occurs when they are arranged in an equilateral triangle. The minimal-energy solution of the Skyrme model in the  $B = 12$  sector has  $C_{3v}$  symmetry, but there is a solution of very slightly higher energy with a larger  $D_{3h}$  symmetry, which is a saddle point and not a local energy minimum. Both have an equilateral triangle shape. Here, we quantize the  $D_{3h}$ -symmetric solution (see Fig. 8), which we believe provides a physically more realistic picture of the nucleus. A more refined analysis might include an anharmonic vibrational mode centered on the  $D_{3h}$ -symmetric solution and oscillating through two  $C_{3v}$ -symmetric minima. This solution can be approximated using the double rational map ansatz [24]. We use this to determine its FR constraints. The ansatz involves a  $D_{3h}$ -symmetric outer map of degree 11,  $R^{\text{out}}$ , and a spherically symmetric degree 1 inner map,  $R^{\text{in}}$ , together with an overall radial profile function. The maps are [9]:

$$R^{\text{out}}(z) = \frac{z^9 + \alpha z^6 + \beta z^3 + \gamma}{z^2(\gamma z^9 + \beta z^6 + \alpha z^3 + 1)}, \quad (19)$$

$$R^{\text{in}}(z) = -z, \quad (20)$$

where  $\alpha = -2.47$ ,  $\beta = -0.84$ , and  $\gamma = -0.13$ . The orientation of the inner map is chosen so that the  $D_{3h}$  symmetry is realized in a way compatible with the outer map. Both maps satisfy

$$R(e^{i\frac{2\pi}{3}} z) = e^{i\frac{2\pi}{3}} R(z), \quad R(1/z) = 1/R(z). \quad (21)$$

As the baryon number is a multiple of four, the FR signs form the trivial representation of  $D_3$ , and so the FR constraints are [6]

$$e^{i\frac{2\pi}{3} L_3} e^{i\frac{2\pi}{3} K_3} |\Psi\rangle = |\Psi\rangle, \quad e^{i\pi L_1} e^{i\pi K_1} |\Psi\rangle = |\Psi\rangle. \quad (22)$$

Both maps satisfy the reflection symmetry

$$R(1/\bar{z}) = 1/\overline{R(z)}, \quad (23)$$

TABLE VII. FR-allowed quantum states of the  $B = 12$  Skyrmion (normalized).

$I$	$J^\pi$	Quantum state $ \Psi_{J^\pi, I,  L_3 ,  K_3 }\rangle$
0	$0^+$	$ \Psi_{0^+, 0, 0, 0}\rangle =  0, 0\rangle \otimes  0, 0\rangle$
	$2^+$	$ \Psi_{2^+, 0, 0, 0}\rangle =  2, 0\rangle \otimes  0, 0\rangle$
	$3^-$	$ \Psi_{3^-, 0, 3, 0}\rangle = \frac{1}{\sqrt{2}}( 3, 3\rangle -  3, -3\rangle) \otimes  0, 0\rangle$
	$4^-$	$ \Psi_{4^-, 0, 3, 0}\rangle = \frac{1}{\sqrt{2}}( 4, 3\rangle +  4, -3\rangle) \otimes  0, 0\rangle$
	$4^+$	$ \Psi_{4^+, 0, 0, 0}\rangle =  4, 0\rangle \otimes  0, 0\rangle$
	$5^-$	$ \Psi_{5^-, 0, 3, 0}\rangle = \frac{1}{\sqrt{2}}( 5, 3\rangle -  5, -3\rangle) \otimes  0, 0\rangle$
	$6^-$	$ \Psi_{6^-, 0, 3, 0}\rangle = \frac{1}{\sqrt{2}}( 6, 3\rangle +  6, -3\rangle) \otimes  0, 0\rangle$
	$6^+$	$ \Psi_{6^+, 0, 0, 0}\rangle =  6, 0\rangle \otimes  0, 0\rangle$
1	$1^+$	$ \Psi_{1^+, 1, 1, 1}\rangle = \frac{1}{\sqrt{2}}( 1, 1\rangle \otimes  1, -1\rangle +  1, -1\rangle \otimes  1, 1\rangle)$
		$ \Psi_{1^+, 1, 0, 0}\rangle =  1, 0\rangle \otimes  1, 0\rangle$
	$2^-$	$ \Psi_{2^-, 1, 2, 1}\rangle = \frac{1}{\sqrt{2}}( 2, 2\rangle \otimes  1, 1\rangle -  2, -2\rangle \otimes  1, -1\rangle)$
	$2^+$	$ \Psi_{2^+, 1, 1, 1}\rangle = \frac{1}{\sqrt{2}}( 2, 1\rangle \otimes  1, -1\rangle -  2, -1\rangle \otimes  1, 1\rangle)$
	$3^-$	$ \Psi_{3^-, 1, 3, 0}\rangle = \frac{1}{\sqrt{2}}( 3, 3\rangle +  3, -3\rangle) \otimes  1, 0\rangle$
		$ \Psi_{3^-, 1, 2, 1}\rangle = \frac{1}{\sqrt{2}}( 3, 2\rangle \otimes  1, 1\rangle +  3, -2\rangle \otimes  1, -1\rangle)$
	$3^+$	$ \Psi_{3^+, 1, 1, 1}\rangle = \frac{1}{\sqrt{2}}( 3, 1\rangle \otimes  1, -1\rangle +  3, -1\rangle \otimes  1, 1\rangle)$
		$ \Psi_{3^+, 1, 0, 0}\rangle =  3, 0\rangle \otimes  1, 0\rangle$
	$4^-$	$ \Psi_{4^-, 1, 4, 1}\rangle = \frac{1}{\sqrt{2}}( 4, 4\rangle \otimes  1, -1\rangle -  4, -4\rangle \otimes  1, 1\rangle)$
		$ \Psi_{4^-, 1, 3, 0}\rangle = \frac{1}{\sqrt{2}}( 4, 3\rangle -  4, -3\rangle) \otimes  1, 0\rangle$
		$ \Psi_{4^-, 1, 2, 1}\rangle = \frac{1}{\sqrt{2}}( 4, 2\rangle \otimes  1, 1\rangle -  4, -2\rangle \otimes  1, -1\rangle)$
	$4^+$	$ \Psi_{4^+, 1, 1, 1}\rangle = \frac{1}{\sqrt{2}}( 4, 1\rangle \otimes  1, -1\rangle -  4, -1\rangle \otimes  1, 1\rangle)$
2	$0^+$	$ \Psi_{0^+, 2, 0, 0}\rangle =  0, 0\rangle \otimes  2, 0\rangle$
	$1^-$	$ \Psi_{1^-, 2, 1, 2}\rangle = \frac{1}{\sqrt{2}}( 1, 1\rangle \otimes  2, 2\rangle -  1, -1\rangle \otimes  2, -2\rangle)$
	$1^+$	$ \Psi_{1^+, 2, 1, 1}\rangle = \frac{1}{\sqrt{2}}( 1, 1\rangle \otimes  2, -1\rangle -  1, -1\rangle \otimes  2, 1\rangle)$
	$2^-$	$ \Psi_{2^-, 2, 1, 2}\rangle = \frac{1}{\sqrt{2}}( 2, 1\rangle \otimes  2, 2\rangle +  2, -1\rangle \otimes  2, -2\rangle)$
		$ \Psi_{2^-, 2, 2, 1}\rangle = \frac{1}{\sqrt{2}}( 2, 2\rangle \otimes  2, 1\rangle +  2, -2\rangle \otimes  2, -1\rangle)$
	$2^+$	$ \Psi_{2^+, 2, 2, 2}\rangle = \frac{1}{\sqrt{2}}( 2, 2\rangle \otimes  2, -2\rangle +  2, -2\rangle \otimes  2, 2\rangle)$
		$ \Psi_{2^+, 2, 1, 1}\rangle = \frac{1}{\sqrt{2}}( 2, 1\rangle \otimes  2, -1\rangle +  2, -1\rangle \otimes  2, 1\rangle)$
		$ \Psi_{2^+, 2, 0, 0}\rangle =  2, 0\rangle \otimes  2, 0\rangle$

and so the parity operator is equivalent to  $\mathcal{P} = e^{i\pi L_3} e^{i\pi K_3}$ . The  $D_{3h}$  symmetry implies that the inertia tensors are diagonal, with  $U_{11} = U_{22}$ ,  $V_{11} = V_{22}$ , and  $W_{11} = W_{22}$ , so the quantum Hamiltonian is that of a system of coupled symmetric tops:

$$H = \left( \frac{U_{11} - W_{11}}{2\Delta_{11}} \right) \mathbf{J}^2 + \left( \frac{V_{11} - W_{11}}{2\Delta_{11}} \right) \mathbf{I}^2 + \left( \frac{W_{11}}{2\Delta_{11}} \right) \mathbf{M}^2 \\ + \left( \frac{U_{33}}{2\Delta_{33}} - \frac{U_{11}}{2\Delta_{11}} \right) L_3^2 + \left( \frac{V_{33}}{2\Delta_{33}} - \frac{V_{11}}{2\Delta_{11}} \right) K_3^2 \\ + \left( \frac{W_{33}}{\Delta_{33}} - \frac{W_{11}}{\Delta_{11}} \right) L_3 K_3, \quad (24)$$

where  $\mathbf{M} = \mathbf{L} + \mathbf{K}$ ,  $\Delta_{33}$  is as before and  $\Delta_{11} = U_{11}V_{11} - W_{11}^2$ .

The states that are allowed by the FR constraints are listed in Table VII. Each of the allowed isospin 0 states is also an eigenstate of the Hamiltonian, and their quantum energies

$E_{J^\pi, I, |L_3|, |K_3|}$  are:

$$\begin{aligned}
 E_{0^+, 0, 0, 0} &= 0, \\
 E_{2^+, 0, 0, 0} &= 3U_{11}/\Delta_{11}, \\
 E_{3^-, 0, 3, 0} &= 3U_{11}/2\Delta_{11} + 9U_{33}/2\Delta_{33}, \\
 E_{4^-, 0, 3, 0} &= 11U_{11}/2\Delta_{11} + 9U_{33}/2\Delta_{33}, \\
 E_{4^+, 0, 0, 0} &= 10U_{11}/\Delta_{11}, \\
 E_{5^-, 0, 3, 0} &= 21U_{11}/2\Delta_{11} + 9U_{33}/2\Delta_{33}, \\
 E_{6^-, 0, 3, 0} &= 33U_{11}/2\Delta_{11} + 9U_{33}/2\Delta_{33}, \\
 E_{6^+, 0, 0, 0} &= 21U_{11}/\Delta_{11}, \\
 E_{6^+, 0, 6, 0} &= 3U_{11}/\Delta_{11} + 18U_{33}/\Delta_{33}.
 \end{aligned} \tag{25}$$

These states also result from the rigid-body quantization of an equilateral triangle with  $\alpha$  particles at its vertices and are not a prediction characteristic of the Skyrme model itself. The states fall into rotational bands labeled by  $|L_3| = 0, 3, 6, \dots$ . As in Refs. [25,26], we suggest that the second experimental  $2^-$  state of carbon-12 at 13.4 MeV has been misidentified and is really a  $4^-$  state. Again as in Ref. [25], we predict a relatively low-energy  $6^+$  state of carbon-12, with  $|L_3| = 6$ . Such a state has not yet been seen experimentally.

The isospin 1 states in Table VII are not all individually eigenstates of the Hamiltonian, as they are not eigenstates of  $\mathbf{M}^2$ . It is convenient to introduce basis states  $|J, I; M, M_3\rangle$  and express the states we have in terms of these. For example, for the two orthonormal FR-allowed  $1^+$  states:

$$\begin{aligned}
 |\Psi_{1^+, 1, 0, 0}\rangle &\equiv |1, 0\rangle \otimes |1, 0\rangle \\
 &= \sqrt{\frac{2}{3}}|1, 1; 2, 0\rangle - \sqrt{\frac{1}{3}}|1, 1; 0, 0\rangle,
 \end{aligned} \tag{26}$$

$$\begin{aligned}
 |\Psi_{1^+, 1, 1, 1}\rangle &\equiv \frac{1}{\sqrt{2}}(|1, 1\rangle \otimes |1, -1\rangle + |1, -1\rangle \otimes |1, 1\rangle) \\
 &= \sqrt{\frac{1}{3}}|1, 1; 2, 0\rangle + \sqrt{\frac{2}{3}}|1, 1; 0, 0\rangle.
 \end{aligned} \tag{27}$$

Neither is an eigenstate of the Hamiltonian, as neither is an eigenstate of  $\mathbf{M}^2$ , but we can find two linear combinations of  $|\Psi_{1^+, 1, 0, 0}\rangle$  and  $|\Psi_{1^+, 1, 1, 1}\rangle$  that are eigenstates by diagonalizing a matrix Hamiltonian. Their energies are the eigenvalues of the  $2 \times 2$  matrix

$$\begin{aligned}
 &\begin{pmatrix} \langle \Psi_{1^+, 1, 0, 0} | H | \Psi_{1^+, 1, 0, 0} \rangle & \langle \Psi_{1^+, 1, 0, 0} | H | \Psi_{1^+, 1, 1, 1} \rangle \\ \langle \Psi_{1^+, 1, 1, 1} | H | \Psi_{1^+, 1, 0, 0} \rangle & \langle \Psi_{1^+, 1, 1, 1} | H | \Psi_{1^+, 1, 1, 1} \rangle \end{pmatrix} \\
 &\equiv \begin{pmatrix} a & c \\ c & b \end{pmatrix},
 \end{aligned} \tag{28}$$

where

$$a = U_{11}/\Delta_{11} + V_{11}/\Delta_{11}, \tag{29}$$

$$b = U_{11}/2\Delta_{11} + V_{11}/2\Delta_{11} + U_{33}/2\Delta_{33} + V_{33}/2\Delta_{33} - W_{33}/\Delta_{33}, \tag{30}$$

$$c = \sqrt{2}W_{11}/\Delta_{11}. \tag{31}$$

The eigenvalues are  $\frac{1}{2}(a + b \pm \sqrt{a^2 + b^2 - 2ab + 4c^2})$ . There are two possible interpretations. Either the energies are close together and remain below the isospin 1 states of higher

spin, in which case we predict two close  $1^+$  states (which have experimentally not been resolved) or their energies are well separated, in which case we predict the observed  $1^+$  state and a higher excited  $1^+$  state that has not yet been seen. From our numerical values for  $a$ ,  $b$ , and  $c$  we calculate the energies to be 0.00194 and 0.00207, which are in fact close together. So we predict that the single observed  $1^+$  isotriplet of states is really an unresolved doublet of isotriplets.

This matrix diagonalization method is also used to calculate the energy eigenvalues for the other values of  $J^\pi$  and  $I$  for which there is more than one allowed state. It is found that in all cases, the off-diagonal elements of the matrices analogous to (28) are small, of the order  $10^{-2}$  times the diagonal elements. We may therefore consistently assign values of  $|L_3|$  and  $|K_3|$  to each of our calculated energy eigenvalues, as the “mixing” of states with the same values of  $J^\pi$  and  $I$ , but different  $|L_3|$  and  $|K_3|$  values, is minimal. The quantum energies of the spin 2 states with isospin 1 are:

$$\begin{aligned}
 E_{2^-, 1, 2, 1} &= U_{11}/\Delta_{11} + 2U_{33}/\Delta_{33} + V_{11}/2\Delta_{11} \\
 &\quad + V_{33}/2\Delta_{33} + 2W_{33}/\Delta_{33},
 \end{aligned} \tag{32}$$

$$\begin{aligned}
 E_{2^+, 1, 1, 1} &= 5U_{11}/2\Delta_{11} + U_{33}/2\Delta_{33} + V_{11}/2\Delta_{11} \\
 &\quad + V_{33}/2\Delta_{33} - W_{33}/\Delta_{33}.
 \end{aligned} \tag{33}$$

We calculate that  $E_{2^-, 1, 2, 1}$  and  $E_{2^+, 1, 1, 1}$  are 0.00218 and 0.00228, respectively, and so the  $2^+$  isotriplet lies above the  $2^-$  isotriplet. Experimentally, however, the  $2^+$  isotriplet is observed below the  $2^-$  isotriplet.

The quantum energies of the isospin 2 states with spins 0 and 1 are:

$$E_{0^+, 2, 0, 0} = 3V_{11}/\Delta_{11}, \tag{34}$$

$$\begin{aligned}
 E_{1^-, 2, 1, 2} &= U_{11}/2\Delta_{11} + U_{33}/2\Delta_{33} + V_{11}/\Delta_{11} \\
 &\quad + 2V_{33}/\Delta_{33} + 2W_{33}/\Delta_{33},
 \end{aligned} \tag{35}$$

$$\begin{aligned}
 E_{1^+, 2, 1, 1} &= U_{11}/2\Delta_{11} + U_{33}/2\Delta_{33} + 5V_{11}/2\Delta_{11} \\
 &\quad + V_{33}/2\Delta_{33} - W_{33}/\Delta_{33}.
 \end{aligned} \tag{36}$$

We calculate these values to be 0.00569, 0.00541, and 0.00574, respectively, and so the  $1^-$  state lies below the  $0^+$  state and the  $1^+$  state lies above the  $0^+$  state. Between the  $0^+$  and  $1^+$  states there is a further  $2^+$  state. Experimentally the  $0^+$  isospin 2 quintet includes the ground states of beryllium-12 and oxygen-12; low-energy excited  $1^-$  and  $2^+$  states of beryllium-12 are also observed. The energy levels of the quantized  $B = 12$  Skyrmion are listed in Table VIII. The experimental spectrum is in Fig. 9.

### A. Three cube interpretation

In Ref. [4] we estimated the moments of inertia of the  $B = 8$  Skyrmion by treating it as a “double cube” of two cubic  $B = 4$  Skyrmions, separated a certain distance along a common  $C_4$  axis, with the cubes rotated around this axis by  $\pi/2$  relative to each other. This enabled us to estimate the energies of the Skyrmion’s quantum states. These estimates agree well with our results using the exact  $B = 8$  solution. In this section we apply a similar procedure to the  $B = 12$  Skyrmion.

We work with three  $B = 4$  cubes arranged in an equilateral triangle, meeting at a common edge. Each cube is related to

TABLE VIII. Energy levels of the  $B = 12$  Skyrmion, using both the exact solution and the three cube interpretation. To each of the quantum states of the exact solution there correspond dominant values of  $|L_3|$  and  $|K_3|$ .

$I$	$J^\pi$	$ L_3 $	$ K_3 $	$E^{\text{exact}}$ ( $\times 10^{-4}$ )	$E^{\text{3-cube}}$ ( $\times 10^{-4}$ )	$E^{\text{exact}}$ (MeV)	$E^{\text{3-cube}}$ (MeV)
0	$0^+$	0	0	0.0	0.0	0.0	0.0
	$2^+$	0	0	5.1	5.2	3.2	3.2
	$3^-$	3	0	7.6	7.6	4.7	4.7
	$4^-$	3	0	14.4	14.5	8.9	9.0
	$4^+$	0	0	17.0	17.4	10.6	10.8
	$5^-$	3	0	22.9	23.2	14.2	14.4
	$6^-$	3	0	33.1	33.7	20.6	20.9
	$6^+$	6	0	25.3	25.2	15.7	15.7
		0	0	35.7	36.5	22.2	22.7
1	$1^+$	1	1	19.4	18.4	12.1	11.5
		0	0	20.7	20.2	12.9	12.6
	$2^-$	2	1	21.8	21.0	13.5	13.0
	$2^+$	1	1	22.8	21.9	14.2	13.6
	$3^-$	3	0	26.4	26.1	16.4	16.2
		2	1	27.0	26.2	16.8	16.3
	$3^+$	1	1	27.8	27.1	17.3	16.9
		0	0	29.3	28.9	18.2	18.0
	$4^-$	4	1	30.6	29.4	19.0	18.2
		3	0	33.1	33.1	20.6	20.5
		2	1	33.9	33.1	21.1	20.6
	$4^+$	1	1	34.7	34.1	21.6	21.2
2	$0^+$	0	0	56.9	55.5	35.4	34.5
	$1^-$	1	2	54.1	50.9	33.6	31.7
	$1^+$	1	1	57.4	55.4	35.7	34.5
	$2^-$	1	2	57.5	54.4	35.7	33.8
		2	1	59.7	58.0	37.1	36.0
	$2^+$	2	2	57.1	53.5	35.5	33.2
		1	1	60.6	58.9	37.7	36.6
		0	0	62.3	60.7	38.7	37.7

its neighbor by a spatial rotation by  $2\pi/3$  followed by an isorotation by  $2\pi/3$ . The isorotation cyclically permutes the values of the pion fields on the faces of the cubes, so that these values match on touching faces. We denote by  $d$  the distance between the center of each cube and the center of the triangle. In a similar manner to the case of the  $B = 8$  double cube, we use the parallel axis theorem to make estimates for the moments of inertia of the  $D_{3h}$ -symmetric  $B = 12$  Skyrmion in terms of the moments of inertia of the  $B = 4$  Skyrmion and the separation parameter  $d$ . We use the quadratic interpolation method to obtain values for the  $B = 4$  inertia tensors with  $m = 0.685$ , the optimized value of  $m$  for the  $B = 12$  sector of the model (see Table I), to obtain the estimates

$$U_{11}^{(B=12)} = U_{22}^{(B=12)} = 3U_{11}^{(B=4)} = 540, \quad (37)$$

$$U_{33}^{(B=12)} = 3U_{33}^{(B=4)} = 645, \quad (38)$$

$$V_{11}^{(B=12)} = V_{22}^{(B=12)} = 3V_{11}^{(B=4)} + \frac{3}{2}\mathcal{M}_4 d^2, \quad (39)$$

$$V_{33}^{(B=12)} = 3V_{11}^{(B=4)} + 3\mathcal{M}_4 d^2. \quad (40)$$

The interpolated value of  $\mathcal{M}_4$  for  $m = 0.685$  is 589.3. The value of  $d$  is chosen using a least-squares method so that our approximation to  $V_{ij}$  is closest to that of the exact  $B = 12$  solution. This yields a value for  $d$  of 1.92 and hence the estimates

$$V_{11}^{(B=12)} = 5756, \quad (41)$$

$$V_{33}^{(B=12)} = 9014. \quad (42)$$

In this simplified picture,  $W_{ij}$  vanishes, as it vanishes for the  $B = 4$  cube. Comparing these numbers to those obtained from the exact solution for  $B = 12$  (given in Appendix A5), we see that the three cube approach has provided good estimates of the inertia tensors  $U_{ij}$  and  $V_{ij}$ , and the inequalities that are satisfied by their elements are right. For the exact solution,  $W_{ij}$  is nonzero but small. Also, for the exact solution the ratio of  $U_{11}$  to  $U_{33}$  is closer to 1 than for the  $B = 4$  cube. This is because the triangular arrangement of the three cubes is closer to the Skyrme crystal, for which  $U_{11} = U_{33}$ . The accuracy of this approximate inertia tensor shows that the Skyrme model is consistent with the intrinsic shape of carbon-12 being an equilateral triangle of three  $\alpha$  particles.

The assumption that  $W_{ij}$  vanishes simplifies the quantum Hamiltonian to the sum of a symmetric top in space and a symmetric top in isospace:

$$H = \frac{1}{2V_{11}}\mathbf{J}^2 + \frac{1}{2U_{11}}\mathbf{I}^2 + \left(\frac{1}{2V_{33}} - \frac{1}{2V_{11}}\right)L_3^2 + \left(\frac{1}{2U_{33}} - \frac{1}{2U_{11}}\right)K_3^2. \quad (43)$$

$|L_3|$  and  $|K_3|$  become good quantum numbers, and the expressions for a selection of the quantum energies simplify to:

$$\begin{aligned} E_{0^+,0,0,0} &= 0, \\ E_{2^+,0,0,0} &= 3/V_{11}, \\ E_{3^-,0,3,0} &= 3/2V_{11} + 9/2V_{33}, \\ E_{4^-,0,3,0} &= 11/2V_{11} + 9/2V_{33}, \\ E_{4^+,0,0,0} &= 10/V_{11}, \\ E_{5^-,0,3,0} &= 21/2V_{11} + 9/2V_{33}, \\ E_{6^-,0,3,0} &= 33/2V_{11} + 9/2V_{33}, \\ E_{6^+,0,0,0} &= 21/V_{11}, \\ E_{6^+,0,6,0} &= 3/V_{11} + 18/V_{33}, \\ E_{1^+,1,1,1} &= 1/V_{11} + 1/U_{11}, \\ E_{1^+,1,0,0} &= 1/2V_{11} + 1/2V_{33} + 1/2U_{11} + 1/2U_{33}, \\ E_{2^-,1,2,1} &= 1/V_{11} + 2/V_{33} + 1/2U_{11} + 1/2U_{33}, \\ E_{2^+,1,1,1} &= 5/2V_{11} + 1/2V_{33} + 1/2U_{11} + 1/2U_{33}, \\ E_{0^+,2,0,0} &= 3/U_{11}, \\ E_{1^-,2,1,2} &= 1/2V_{11} + 1/2V_{33} + 1/U_{11} + 2/U_{33}, \\ E_{1^+,2,1,1} &= 1/2V_{11} + 1/2V_{33} + 5/2U_{11} + 1/2U_{33}, \\ E_{2^+,2,2,2} &= 1/V_{11} + 2/V_{33} + 1/U_{11} + 2/U_{33}. \end{aligned} \quad (44)$$

Their numerical values (using  $U_{11} = 540$ ,  $U_{33} = 645$ ,  $V_{11} = 5756$ , and  $V_{33} = 9014$ ) are listed in Table VIII alongside the corresponding values using the exact solution. We also present the values in physical units, obtained using the  $B = 12$  parameter set given in Table I.



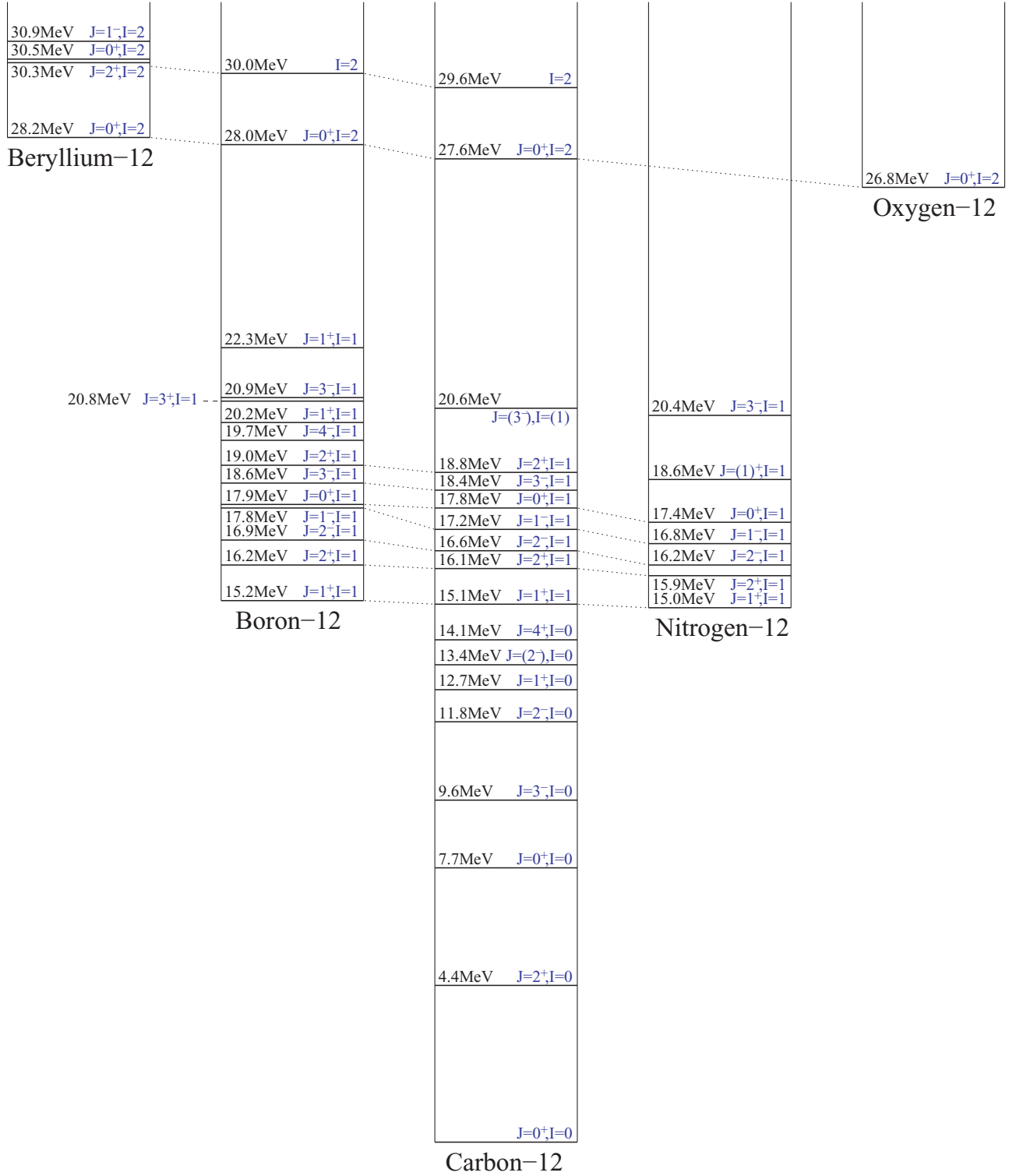


FIG. 9. (Color online) Energy level diagram for nuclei of mass number 12. Mass splittings between nuclei are adjusted to eliminate the proton/neutron mass difference and remove Coulomb effects, as described in Ref. [27].

### B. Comparison with experimental data

The ground state of carbon-12 is a  $0^+$  state with isospin 0. It has excited  $2^+$ ,  $3^-$ , and  $4^+$  states with excitation energies 4.4, 9.6, and 14.1 MeV, respectively. In addition, there may be a  $4^-$  state at 13.4 MeV (reassigned from the  $2^-$  state at this energy).

As can be seen from Table VIII, we predict precisely these states and in the same order. Our predictions for their excitation energies are 3.2, 4.7, 10.6, and 8.9 MeV, respectively.

Carbon-12 has an excited  $0^+$  state at 7.7 MeV, the famous Hoyle state. Unfortunately, our method of rigid-body

quantization prohibits two independent spin 0, isospin 0 states. An extension of the model might allow this. Perhaps the lowest-lying quantum state of an alternative  $B = 12$  solution, such as the  $C_{3v}$ -symmetric solution, or a solution with three  $B = 4$  Skyrmions in a linear chain, both discussed in Ref. [9], could be interpreted as this excited  $0^+$  state. Additional excited states of carbon-12 are seen experimentally but are not yet predicted in our model: for example, a  $1^+$  state at 12.7 MeV.

We predict two nondegenerate  $1^+$  states with isospin 1. An isotriplet with  $J^\pi = 1^+$  is observed, which includes the ground states of boron-12 and nitrogen-12, with average excitation energy 15.1 MeV, to be compared to our value of 12.1 MeV. As mentioned previously, this may be an unresolved doublet of isotriplets. However, a number of higher  $1^+$  states with isospin 1 are seen in the nuclear spectra. We also predict a  $2^+$  and a  $2^-$  isotriplet. Both of these are seen experimentally, but in the opposite order: we predict the  $2^-$  isotriplet to lie below the  $2^+$  isotriplet. Experimentally, the  $2^+$  isotriplet has an average excitation energy of 16.1 MeV, compared with 16.5 MeV for the  $2^-$  isotriplet. Higher excited  $1^-$  and  $0^+$  isotriplets are seen experimentally, but we do not predict them in our model. We find two allowed  $3^+$  states with isospin 1, at 17.3 and 18.2 MeV. One such state has been seen in the spectrum of boron-12, at 20.8 MeV. An incomplete  $3^-$  isotriplet is observed at 18.5 MeV, which we predict at 16.4 MeV. We predict a second  $3^-$  state with isospin 1 at 16.8 MeV. States with these quantum numbers are seen in the spectra of boron-12, carbon-12, and nitrogen-12 at 20.9, 20.6, and 20.4 MeV, respectively. A further excited  $4^-$  state of boron-12 with isospin 1 exists at 19.7 MeV, to be compared with our value of 19.0 MeV.

An (incomplete)  $J^\pi = 0^+$ , isospin 2 quintet, which includes the ground states of beryllium-12 and oxygen-12, is observed experimentally with an average excitation energy of 27.7 MeV. We predict such an isoquintet at 35.4 MeV. We also predict the existence of a  $1^-$  isoquintet with an excitation energy less than that of the  $0^+$  isoquintet. Such a  $1^-$  state is observed in beryllium-12, at 2.7 MeV above the  $0^+$  ground state. An (incomplete)  $2^+$  isoquintet is experimentally observed with an average excitation energy roughly 2 MeV above the  $0^+$  isoquintet. In our model three  $2^+$  states with isospin 2 are allowed, just above the  $0^+$  state.

In summary, the model describes the energy spectra of nuclei of mass number 12 especially well. The rotational band of carbon-12 is very well reproduced, along with some of the experimentally observed isospin 1 triplets and isospin 2 quintets. However, the observed isotriplets with  $J^\pi = 0^+$  and  $1^-$  do not appear as quantum states of our  $D_{3h}$ -symmetric Skyrmion (neither does the Hoyle state). They may arise from the quantization of further modes or appear as quantum states of an alternative Skyrmion. The molecular rotational band of beryllium-12 in the range 10–20 MeV above the beryllium-12 ground state [28] may also be explained in terms of an alternative Skyrmion.

### VIII. CONCLUSION

The Skyrme model provides a model of nuclei that unifies spin and isospin as collective excitations of topological

solitons. We have been able to reproduce the energy spectra of a number of light nuclei to a good degree of accuracy by quantizing Skyrmions as rigid bodies in space and isospace and by parametrizing the model separately for each mass number. The model is fitted to nuclear charge radii and masses. Remarkably, this leads to good predictions for moments of inertia, spin splittings, and isobar splittings. The quantum states we have calculated agree well with what is experimentally observed, with the correct spins and parities. Among the successes of the model is the prediction of the existence and the excitation energies of the rotational bands of beryllium-8 and carbon-12. We predict that neither beryllium-10 nor carbon-10 has a  $1^+$  state, in agreement with experiment. Our predictions of the quantum states of the nuclear isobars with nonzero isospin is quantitatively good, and the spin splittings are quite good. However, the spin states do not always appear in the correct order. A few, so far unobserved, states have been predicted, notably some negative-parity states of lithium-8 and boron-8 and some high-spin states, including a  $4^+$  state of helium-4 and a  $6^+$  state of carbon-12. Several observed states are not predicted by the rigid-body quantization of Skyrmions. To understand these one will need to consider further Skyrmion degrees of freedom.

One can be pleased with the general trend of isospin excitations. In each case, the  $I = 0, 1$  splitting is of the order of 10 MeV, the  $I = 0, 2$  splitting of the order of 20–30 MeV, and the  $I = 0, 3$  splitting of the order of 60 MeV. Isospin splittings for spherically averaged Skyrmions, over a wider range of baryon numbers and isospins, have been estimated in Ref. [29]. The Skyrme model predicts that the isobar splittings rise in proportion to  $I(I + 1)$ . Curiously the experimental data do not rise quite as fast, but our prediction for the coefficient of  $I(I + 1)$  is roughly correct.

It would have been possible to have chosen just one parameter set, as in previous work [4]. We could have chosen  $m$  close to 1, the energy scale close to 6 MeV, and the length scale close to 1.6 fm, for example. This would have provided good qualitative results but would not have given such a good fit to charge radii and energy splittings.

Further work is needed on the electromagnetic form factors and transition amplitudes of light nuclei within the Skyrme model, as these provide more information about the internal structure of nuclei. It would also be desirable to consider the effect of vibrational modes and the breakup of Skyrmions into clusters, for example, modeling the breakup of lithium-6 into helium-4 and the deuteron. Finally, we would like to extend this analysis to Skyrmions and nuclei with  $B = 7, 9, 11$ , and beyond 12.

### ACKNOWLEDGMENTS

N.S.M. and P.M.S. thank STFC for support under rolling Grants ST/G000581/1 and ST/G000433/1. S.W.W. would also like to thank STFC for financial support. The parallel computations were performed on COSMOS at the National Cosmology Supercomputing Centre in Cambridge, UK.

**APPENDIX A: NUMERICAL RESULTS**

The static energies, mean charge radii, and nonzero elements of the inertia tensors for  $B = 4, 6, 8, 10$ , and 12 have been calculated for  $m = 0.5, 1$ , and 1.5 and are shown below. The interpolated values for the preferred values of  $m$  are shown in the final columns. An estimate of the numerical errors can be made by calculating the off-diagonal inertia tensor elements, which should be identically zero in each case. The calculated ratio of off-diagonal elements to nonzero diagonal elements is of the order of  $10^{-2}$  or less.

**A1.  $B = 4$** 

	$m = 0.5$	$m = 1$	$m = 1.5$	$m = 0.820$
$U_{11}$	201	151	124	167
$U_{33}$	241	180	146	198
$V_{33}$	928	701	576	771
$\langle r^2 \rangle^{1/2}$	1.679	1.360	1.185	1.458
$\mathcal{M}_4$	569	624	681	604

**A2.  $B = 6$** 

	$m = 0.5$	$m = 1$	$m = 1.5$	$m = 1.153$
$U_{11}$	305	228	186	211
$U_{33}$	329	245	199	227
$V_{11}$	2195	1658	1362	1542
$V_{33}$	1927	1451	1190	1349
$W_{33}$	-105	-84	-71	-79
$\langle r^2 \rangle^{1/2}$	1.948	1.620	1.430	1.547
$\mathcal{M}_6$	858	946	1036	973

**A3.  $B = 8$** 

	$m = 0.5$	$m = 1$	$m = 1.5$	$m = 0.832$
$U_{11}$	403	299	243	329
$U_{22}$	374	291	242	315
$U_{33}$	418	326	271	353
$V_{11}$	4740	4052	3490	4269
$V_{33}$	1990	1390	1109	1556
$\langle r^2 \rangle^{1/2}$	2.316	2.017	1.787	2.109
$\mathcal{M}_8$	1106	1213	1323	1177

**A4.  $B = 10$** 

	$m = 0.5$	$m = 1$	$m = 1.5$	$m = 0.830$
$U_{11}$	511	383	303	421
$U_{22}$	508	380	298	418
$U_{33}$	459	351	285	383
$V_{11}$	4250	3120	2360	3463
$V_{22}$	5860	4520	3700	4917
$V_{33}$	5730	4400	3590	4794
$W_{33}$	-10.4	-4.8	0.7	-6.7
$\langle r^2 \rangle^{1/2}$	2.455	2.047	1.745	2.174
$\mathcal{M}_{10}$	1373	1516	1657	1468

**A5.  $B = 12$** 

	$m = 0.5$	$m = 1$	$m = 1.5$	$m = 0.685$
$U_{11}$	588	444	364	527
$U_{33}$	653	500	396	590
$V_{11}$	6487	5037	4087	5891
$V_{33}$	9743	7684	6240	8909
$W_{11}$	-49	-40	-37	-45
$W_{33}$	-42	-35	-40	-38
$\langle r^2 \rangle^{1/2}$	2.674	2.265	1.952	2.511
$\mathcal{M}_{12}$	1653	1816	1982	1713

**APPENDIX B: QUADRATIC INTERPOLATION BETWEEN THREE POINTS**

To obtain approximations to the inertia tensors, static energies, and mean charge radii for a given value of  $m$ , we use the method of quadratic interpolation between three points. We know the values of a property  $p$  at  $m = 0.5, 1$ , and 1.5, and we make the ansatz

$$p(m) = \alpha_1 + \alpha_2 m + \alpha_3 m^2. \quad (\text{B1})$$

Let  $\mathbf{p} = (p(0.5), p(1), p(1.5))^T$ . The vector  $\boldsymbol{\alpha} = (\alpha_1, \alpha_2, \alpha_3)^T$  is obtained by inverting the expression

$$\mathbf{M} \cdot \boldsymbol{\alpha} = \mathbf{p}, \quad (\text{B2})$$

where

$$\mathbf{M} = \begin{pmatrix} 1 & 0.5 & 0.25 \\ 1 & 1 & 1 \\ 1 & 1.5 & 2.25 \end{pmatrix},$$

and therefore

$$\mathbf{M}^{-1} = \begin{pmatrix} 3 & -3 & 1 \\ -5 & 8 & -3 \\ 2 & -4 & 2 \end{pmatrix}. \quad (\text{B3})$$

The interpolated values are given in the right-hand columns of the tables in Appendices A1 to A5.

- [1] T. H. R. Skyrme, Proc. R. Soc. A **260**, 127 (1961).
- [2] N. Manton and P. Sutcliffe, *Topological Solitons* (Cambridge University Press, Cambridge, 2004).
- [3] E. Braaten and L. Carson, Phys. Rev. D **38**, 3525 (1988).
- [4] O. V. Manko, N. S. Manton, and S. W. Wood, Phys. Rev. C **76**, 055203 (2007).
- [5] D. Finkelstein and J. Rubinstein, J. Math. Phys. **9**, 1762 (1968).
- [6] S. Krusch, Ann. Phys. **304**, 103 (2003).
- [7] R. A. Battye and P. M. Sutcliffe, Phys. Rev. Lett. **79**, 363 (1997).
- [8] R. A. Battye and P. M. Sutcliffe, Phys. Rev. C **73**, 055205 (2006).
- [9] R. A. Battye, N. S. Manton, and P. M. Sutcliffe, Proc. R. Soc. A **463**, 261 (2007).
- [10] N. S. Manton and S. W. Wood, Phys. Rev. D **74**, 125017 (2006).
- [11] C. J. Houghton, N. S. Manton, and P. M. Sutcliffe, Nucl. Phys. **B510**, 507 (1998).
- [12] R. A. Battye, S. Krusch, and P. M. Sutcliffe, Phys. Lett. **B626**, 120 (2005).
- [13] G. S. Adkins, C. R. Nappi, and E. Witten, Nucl. Phys. **B228**, 552 (1983).
- [14] G. S. Adkins and C. R. Nappi, Nucl. Phys. **B233**, 109 (1984).
- [15] L. D. Landau and E. M. Lifshitz, *Quantum Mechanics—Course of Theoretical Physics*, 3rd ed. (Butterworth-Heinemann, Oxford, 1977), Vol. 3.
- [16] F. Meier and H. Walliser, Phys. Rep. **289**, 383 (1997).
- [17] T. S. Walhout, Nucl. Phys. **A547**, 423 (1992).
- [18] D. R. Tilley, H. R. Weller, and G. M. Hale, Nucl. Phys. **A541**, 1 (1992).
- [19] D. R. Tilley *et al.*, Nucl. Phys. **A708**, 3 (2002).
- [20] D. R. Tilley *et al.*, Nucl. Phys. **A745**, 155 (2004).
- [21] B. Aubert *et al.*, Phys. Rev. Lett. **101**, 071801 (2008).
- [22] R. Partridge *et al.*, Phys. Rev. Lett. **45**, 1150 (1980).
- [23] P. Navrátil and E. Caurier, Phys. Rev. C **69**, 014311 (2004).
- [24] N. S. Manton and B. M. A. G. Piette, in *European Congress of Mathematics, Barcelona, 10–14 July 2000*, edited by C. Casacuberta *et al.* (Birkhäuser, Basel, 2001), Vol. I; Prog. Math. **201**, 469 (2001).
- [25] R. Álvarez-Rodríguez, E. Garrido, A. S. Jensen, D. V. Fedorov, and H. O. U. Fynbo, Eur. Phys. J. A **31**, 303 (2007).
- [26] R. Álvarez-Rodríguez, A. S. Jensen, D. V. Fedorov, and H. O. U. Fynbo, Int. J. Mod. Phys. E **17**, 2188 (2008).
- [27] F. Ajzenberg-Selove, Nucl. Phys. **A506**, 1 (1990).
- [28] W. von Oertzen, M. Freer, and Y. Kanada-En'yo, Phys. Rep. **432**, 43 (2006).
- [29] V. B. Kopeliovich, A. M. Shunderuk, and G. K. Matushko, Phys. At. Nucl. **69**, 120 (2006).